

Electrostatic degrees of freedom in non-Maxwellian plasma^{a)}

F. Skiff,^{b)} H. Gunell, A. Bhattacharjee, C. S. Ng, and W. A. Noonan
Department of Physics and Astronomy, University of Iowa, Iowa City, Iowa 52242

(Received 2 November 2001; accepted 24 January 2002)

Detailed measurements of the ion velocity distribution function are used to test representations of the electrostatic degrees of freedom of slightly non-Maxwellian plasmas. It is found that fluid theory does not describe the data very well because there exist multiple closely spaced kinetic electrostatic modes. New wave branches appear that theoretically should persist as weakly damped modes even with $T_e \sim T_i$. Both a sum over discrete dispersion relations and the Case–Van Kampen spectral representation can be used to provide working descriptions of the data, but the latter has certain advantages. © 2002 American Institute of Physics. [DOI: 10.1063/1.1462031]

I. INTRODUCTION

Collective modes are the primary degrees of freedom in high-temperature plasmas. Because of Debye shielding, discrete particle effects are ignorable in the limit of classical plasma. Therefore, plasma electrostatic degrees of freedom consist of collective dynamical perturbations where shielding does not occur. Consequently, the starting point for descriptions of plasma phenomena is usually to identify the modes that may be active in a given physical situation. Here we report experimental tests of descriptions of ion waves in slightly non-Maxwellian plasma. Under the conditions of the experiment one would expect, based on fluid theory or on kinetic theory with a Maxwellian equilibrium, that only the electrostatic ion cyclotron wave would be observed in the measurements. Instead, multiple discrete modes with dispersion relations $\omega_\alpha(k_\alpha) = \omega$ are observed where ω is the externally applied frequency. These new modes can be found by calculating the dielectric function using the actual measured ion distribution function. Although they are similar in origin to beam modes, multiple modes are found even for slight deviations from a Maxwellian distribution. These kinetic modes can be numerous and are sensitive to details of the ion distribution function. Because the continuous spectrum (Case–Van Kampen modes) is a feature of the Vlasov equation that is not preserved by realistic collision operators, it is not obvious that it can be used to represent data in weakly collisional plasmas.^{1,2} Nevertheless, we find that a representation in terms of the continuum, using Morrison's G-transform, is very useful.³ This representation allows us to determine both the electric field $E(z)$ and the electric displacement $D(z)$ over a large spatial region from measurements of the perturbed ion distribution function at a single location.

It is well known that injection of energetic beams of particles into plasmas can produce unstable modes.⁴ Furthermore, it is known that a two-ion species plasma may exhibit new modes.⁵ Plasmas with two electron temperatures support what are known as electron acoustic modes.^{6,7} We believe

that all of these phenomena are related, but the surprise here is that even a slight modification of the distribution function can be sufficient in order to produce one or more additional weakly damped modes. Instability requires regions of positive slope and significant modifications to the distribution at higher velocity. By comparison, the modifications necessary to activate new weakly-damped modes, even for $T_e \sim T_i$, can be relatively slight. These modifications can also significantly increase the energy density of the waves (for a given level of density fluctuation).

This paper is organized as follows; after a description of the experimental configuration in Sec. II a brief summary of the data and its representation are given in Sec. III. In Sec. IV the description in terms of both discrete dispersion relations and the continuous spectrum are considered. Section V is a brief summary with some comments concerning extensions of this work.

II. EXPERIMENTAL SETUP

The experiments are performed in a uniformly magnetized straight plasma cylinder of diameter 10 cm and length of 200 cm. The magnetic field is along the axis of the cylinder and is 1 kG. A singly ionized Argon plasma of density 10^9 cm^{-3} , electron temperature $T_e \sim 2.5 \text{ eV}$, ion temperature $T_i \sim 0.08 \text{ eV}$, is produced by a radio frequency plasma source (12 MHz, 20 W) at one end of the cylinder. A mesh grid is used to isolate the plasma source frequency (which is in any case well above the ion plasma frequency and the ion wave frequencies) from the main chamber. The pressure of neutral Argon is regulated to 2×10^{-4} Torr in the source region and the plasma is run continuously.

The ion distribution function is measured using laser induced fluorescence (LIF) on the 611 nm metastable absorption ion line with emission at 461 nm. A single frequency scanning dye laser is used to Doppler select the ion velocity parallel to the magnetic field. Thus, the laser beam is aligned parallel to the magnetic field and fluorescence light is collected by an optical periscope that views across the magnetic field (see Fig. 1). Circularly polarized laser light is used so that only one set of the closely spaced Zeeman components of the sigma-polarized absorption lines are involved in the

^{a)}Paper RI2 5, Bull. Am. Phys. Soc. **46**, 290 (2001).

^{b)}Invited speaker.

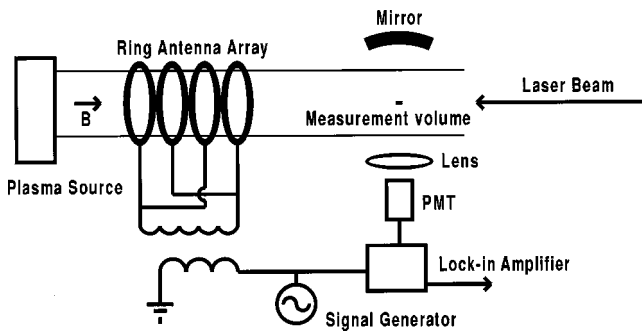


FIG. 1. Experimental setup.

LIF. Remaining Zeeman structure is readily deconvolved by means of a Fast Fourier Transform (FFT). Considerable attention has been given to the design of the optical system in order to achieve high light collection efficiency. Using a chopper to eliminate background collisionally induced fluorescence, signal to noise ratios on the order of 10^4 for the measurement of the total ion distribution function are obtained. Figure 2 shows an ion distribution function from LIF that is typical of the equilibrium state of the plasma. Because the plasma is produced by a source located at one end of the chamber, there is typically a small tail population in the velocity direction out of the source toward the main chamber. The laser beam is introduced on the end of the cylinder opposite to the plasma source.

Perturbations in the ion velocity distribution function $f^1(z, \nu, \omega)$ from an antenna structure on a movable carriage inside the vacuum chamber are studied as a function of the distance z from the antenna structure along the magnetic field. The measurement integrates over velocity components perpendicular to the laser beam (and thus to the magnetic field), but is spatially resolved in all spatial directions to a volume on the plasma cylinder axis defined by the intersection of the laser beam and the periscope viewing volume (roughly a cylinder of diameter and length equal to 0.4 cm aligned on the magnetic field in this experiment). A set of

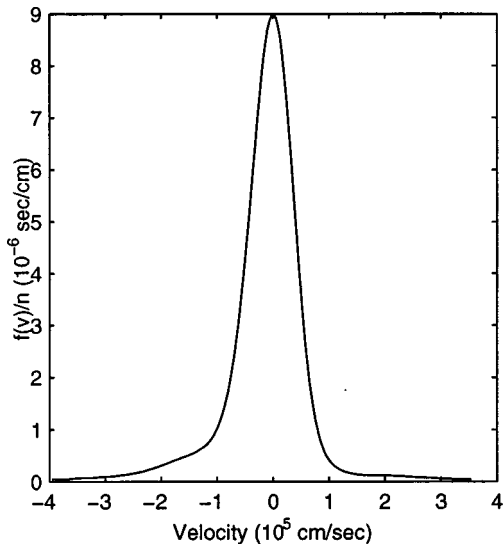


FIG. 2. Equilibrium distribution function measured using LIF.

four rings with relative phase $[0 \ \pi \ 0 \ \pi]$ and spaced by 1 cm are used to excite single frequency (ω) perturbations in the ions. Then, a lock-in amplifier is used to select the time Fourier component of the LIF signal at the frequency of the signal applied to the antenna. Density perturbations are kept small $n^1/n \sim 10^{-2}$ and power spectral density measurements of the LIF signal (without the lock-in) indicate that the plasma response is at the applied frequency. The perturbations are highly asymmetric with respect to propagation direction along the magnetic field. We will concentrate here on the perturbations moving in the same direction as the tail particles.

III. BASIC CHARACTERISTICS OF THE DATA

Apart from the improved signal to noise of the data, the basic characteristics observed in the ion perturbations here are the same as have been reported earlier.^{1,8,9} At most frequencies, the perturbations propagate nearly parallel to the magnetic field and consist of multiple discrete modes with the same frequency and perpendicular wave number. Large data sets exist at 30, 40, 50, 60, and 75 kHz and the ion cyclotron frequency is 38 kHz. At some frequencies ion Bernstein waves are observed at axial locations near the antenna, but they have a negligible influence on the data considered here. Although the existence of discrete modes at the experimentally relevant phase velocities, was found through an analysis of the kinetic equation with a Maxwellian ion distribution, we now understand that the small population of tail ions is crucial to understand the weak damping of these kinetic modes (which we previously could not explain). This also explains why modification of the tail population by ion heating affects the mode structure of the excited waves.⁹

IV. THEORETICAL DESCRIPTIONS

A. Discrete modes

The collisionless magnetized hot-plasma collective-mode dispersion relation $\epsilon(\omega, \mathbf{k})=0$ between the wave angular frequency ω and the wave number components $(k_{\parallel}, k_{\perp})$ parallel and perpendicular, respectively, to the fixed magnetic field for quasineutral electrostatic ion waves can be written for an equilibrium distribution function with definite thermal velocity $v_{t\perp}$ perpendicular to the uniform magnetic field, ion cyclotron frequency Ω_c and ion acoustic speed given by the electron temperature and the ion mass $C_s^2 = T_e / m_i$:

$$1 + \frac{C_s^2}{n} \sum_{j=-\infty}^{\infty} I_j(b) e^{-b} \left\{ K \left(\frac{\partial f}{\partial v} \right) - \frac{j\Omega}{k_{\parallel} v_{t\perp}^2} K(f) \right\}_{u=(1+\Omega_c/\omega)(\omega/k_{\parallel})} = 0. \tag{1}$$

Here $b = (k_{\perp} v_{t\perp} / \Omega_c)^2$, I_n is a modified Bessel function, and we have introduced a factorized velocity distribution function $F(v_{\parallel}, v_{\perp}) = (2\pi v_{t\perp}^2)^{-1} e^{-v_{\perp}^2/2v_{t\perp}^2} f(v_{\parallel})$, where $\int f dv_{\parallel} = n$. The transformation K is related to a Hilbert transform and is sometimes called the ‘‘analytic signal’’:

$$K[h(v)]_u = \pi(H(h) + ih(u)). \tag{2}$$

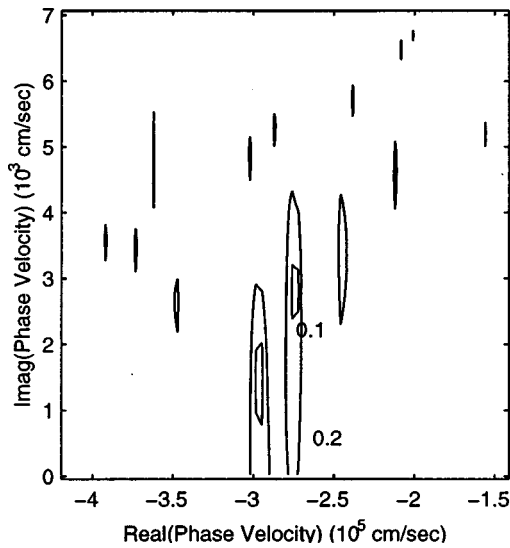


FIG. 3. Contours of the plasma response function $1/|\epsilon(u)|$ in the complex u -plane (50 kHz).

The Hilbert transform is defined as $H(h) \equiv (p/\pi) \int_{-\infty}^{\infty} [\bar{h}(v)/(v-u)] dv$ where the letter p is used to denote the Cauchy principal value of the integral. In the limit of a Maxwellian velocity distribution function one obtains the usual formula in terms of the plasma dispersion function $K[\partial f/\partial v]_{u=\omega/k_{\parallel}} \rightarrow Z(\omega/k_{\parallel})n$. Given experimental measurements of the distribution function f , the dispersion relation (1) can be computed by analytic continuation in the complex u plane (using a FFT). An alternative approach is to use a model function for f that can be fit to experimental data and which permits easy evaluation of the velocity integrals.¹⁰ Either approach reveals the existence of the weakly damped kinetic modes observed in the experiments.

Figure 3 shows contours of the plasma response function $1/|\epsilon|$ in the complex phase velocity plane for the distribution function of Fig. 2 with $k_{\perp}=0$ ($b=0$). Each closed contour encloses the phase velocity of a dispersion relation (and some may be unresolved). Because the Fourier transformed kinetic equation for $k_{\perp}=0$ and $u=\omega/k_{\parallel}$ can be written as

$$(\nu-u)f^1 = C_s^2 \frac{1}{n} \frac{\partial f}{\partial v} \int f^1 dv, \tag{3}$$

the electrostatic dispersion relations for $\omega \ll \omega_{pi}$ are all non-dispersive for parallel propagation. Figure 4 shows the existence of weakly damped modes for the model distribution function of Fig. 5. In this case the modes are plotted in the complex $\kappa = \sqrt{2}k_{\parallel}C_s/\omega$ plane and $T_e = T_i$. The addition of coulomb collisions to the model removes the modes near the origin in Fig. 4 out to large values of imaginary κ .² The weakly damped solutions near $\kappa=0.7$, however, remain weakly damped even with the addition of weak Coulomb collisions. Thus, the conventional wisdom that ion acoustic waves are strongly damped for $T_e = T_i$ is only true for special cases such as the Maxwellian ion distribution function. Because of wave-particle resonance, the perturbations of the ion distribution function are not in phase at all velocities. These

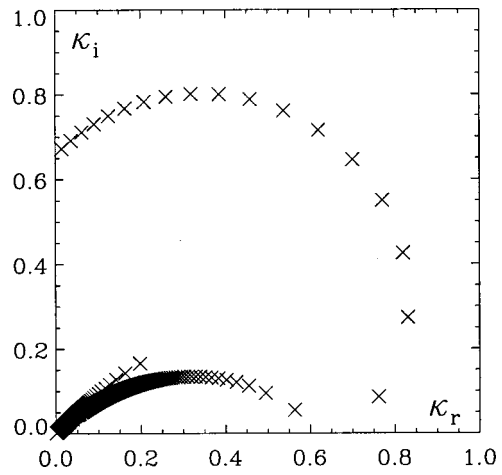


FIG. 4. The ‘‘Landau poles’’; solutions of the dispersion relation in the complex $\kappa = \sqrt{2}k_{\parallel}v_i/\omega$ plane for $T_e = T_i$ and a non-Maxwellian ion distribution.

phase shifts cause the ion distribution function to behave as multiple fluids, depending on the phase velocity of the perturbation. This is the origin of the kinetic modes, which in other respects are very much like ion acoustic waves. A simple three-fluid model that reproduces the dispersion relation of the first kinetic mode is given in the Appendix.

Given the antenna (spatial) spectral amplitude $P(k)$ and the derivative of the dispersion relation it is possible to attempt a prediction of the measured ion perturbation by a sum over the dispersion relations:

$$f^1(z, \nu, \omega) = \sum_{\alpha} \sum_j \frac{C_s^2 \left[\frac{\partial f}{\partial v_{\parallel}} - \frac{j\Omega_c}{k_{\parallel}v_{\perp}^2} f \right] I_j(b) e^{-b}}{\nu - \frac{\omega - j\Omega_c}{k_{\alpha}}} \times e^{ik_{\alpha}z} \frac{P(k_{\alpha})}{\frac{\partial \epsilon}{\partial k_{\alpha}}}. \tag{4}$$

Because the discrete values of k_{α} are complex, the resulting expression can readily be evaluated on the real velocity axis.

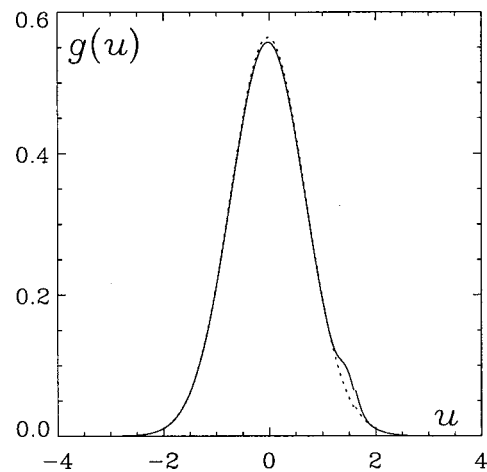


FIG. 5. Ion distribution function producing the dispersion relations in Fig. 4.

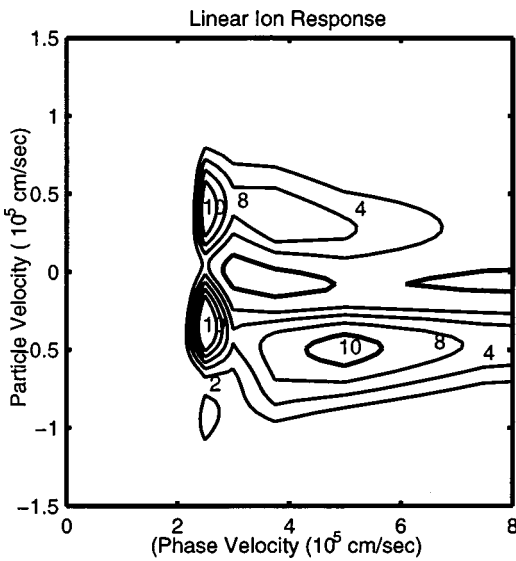


FIG. 6. Contours of the directly measured kinetic mode contribution to magnitude of the perturbed ion distribution function in the particle velocity—phase velocity plane at 40 kHz.

Because of the existence of weakly damped cyclotron harmonic waves at some frequencies it is necessary to keep the effects of $b \neq 0$. For the purpose of a comparison with the data in the ν -particle ν -phase ($=u$) plane the computation of Eq. (4) is subsequently processed in the same way as the experimental data using a spatial FFT to pass from $f^1(z, \nu, \omega)$ to $f^1(k_{\parallel}, \nu, \omega)$ and a change of variable to pass to $f^1(u = \omega/k_{\parallel}, \nu, \omega)$. Contours of the magnitude of this function are plotted as a function of u and ν in Fig. 6 for direct perturbation data. Figure 7 shows a prediction based on Eq. (4). In both cases the contribution of the ion acoustic wave has been removed to make a more clear comparison of the kinetic mode component. It is difficult to improve beyond the qualitative comparison of Figs. 6 and 7 using the sum

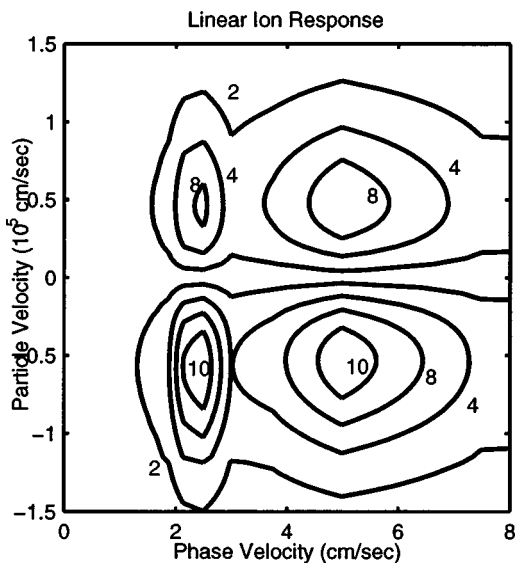


FIG. 7. Prediction of Fig. 6 from an implementation of Eq. (4).

over discrete modes approach because of the difficulty of finding and accurately estimating the excitation of each mode in the complex u plane.

B. The continuous spectrum

For simplicity, we will present here a description of the continuous spectrum in 1-D unmagnetized plasma at low frequency. In actuality there is a series of continuous spectra, one for each cyclotron harmonic, so we will consider situations here where small but nonzero b does not introduce additional weakly damped modes according to Eq. (1). Even with $b = 0$, the wave degrees of freedom of collisionless plasmas are, strictly speaking, infinite. One only obtains a finite set of discrete dispersion relations for waves $\omega(k)$ with additional assumptions of fluid theory, phase-mixing, or by including the effects of collisions.² In other words, collisionless plasmas will support perturbations for any values of ω and k consistent with plasma behavior and for which there are plasma particles moving at the speed $\nu = \omega/k$. This continuum of degrees of freedom is named after Case and Van Kampen (CVK) who independently studied the kinetic theory of electron plasma waves. Ion waves may also be described by starting from the Vlasov and Poisson equations. The difference is that for ion waves at low frequency the electrons form a neutralizing background that is quasi-neutral $n_e \sim n_i$ and the electron density follows a Boltzmann distribution $n_e = n_0 \exp(e\Phi/kT_e)$. It is with these assumptions that we obtain Eq. (3).

A general solution to Eq. (3) can be written as a sum over CVK modes $G(\nu, u)$ with weight function $W(u, \omega)$ (ω can be thought of as a parameter here since we consider monochromatic perturbations):

$$f^1(z, \nu, \omega) = \int W(u, \omega) G(\nu, u) e^{i\omega(z/u)} du. \tag{5}$$

The ion-wave CVK mode is a real singular function:

$$G(\nu, u) = \varepsilon_1(\nu) \delta(\nu - u) + \varepsilon_2(\nu) \frac{p}{\pi} \frac{1}{\nu - u}, \tag{6}$$

$$\varepsilon_1 \equiv \left(1 - C_s^2 p \int \frac{\partial f_0}{\partial v'} \frac{1}{v' - \nu} dv' \right); \quad \varepsilon_2 \equiv \pi C_s^2 \frac{\partial f_0}{\partial v} \frac{1}{n_0}.$$

Integration of Eq. (5) shows that the weight function $W(u, \omega)$ is related to the spatial Fourier transform of the perturbed density:

$$W(u, \omega) = -\frac{\omega}{u^2} n^1 \left(k = \frac{\omega}{u}, \omega \right). \tag{7}$$

Equation (7) indicates that the CVK spectrum W can in principle be determined from measured density fluctuations. It can also be determined from the perturbed distribution function f^1 through a projection onto appropriately normalized adjoint CVK modes:

$$W(u, \omega) e^{i\omega z/u} = \int f^1(u, \nu, \omega) \tilde{G}(u, \nu) d\nu, \tag{8}$$

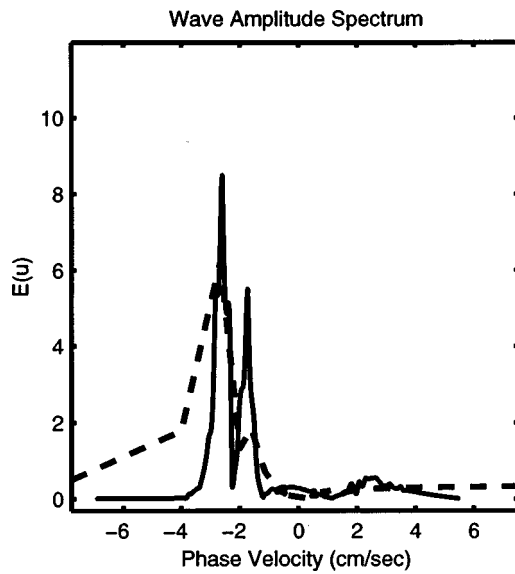


FIG. 8. Magnitude of the electric field spectrum $|E(k)|$ from measurements of the spatial dependence of the density fluctuations (dashed curve) as compared to using the inverse G -transform [Eq. (8)] solid curve at 40 kHz.

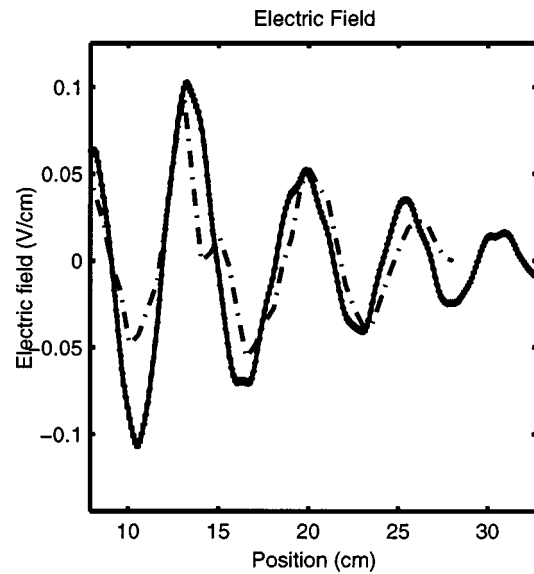


FIG. 9. Comparison of the electric field $E(z)$ calculated from the two methods of Fig. 8.

$$\tilde{G}(u, \nu) = \frac{1}{\varepsilon_1^2(u) + \varepsilon_2^2(u)} \left\{ \varepsilon_1(u) \delta(\nu - u) + \varepsilon_2(u) \frac{p}{\pi} \frac{1}{\nu - u} \right\}. \quad (9)$$

Equations (5) and (8) can be thought of as an integral transform pair or as a variable transformation and were introduced by Morrison (thus we refer to it as Morrison's G -transform).³ Despite the singular functions, these integrals can be conveniently performed on experimental data. Especially for plasmas with $T_e \gg T_i$ it is much easier to determine the spectrum through measurements of phase-space motions rather than total density fluctuations because of quasineutrality. Furthermore, with the assumption that the function W should not have rapid oscillations at small phase velocities (this would correspond to an antenna with complex small scale structure), it is possible to reconstruct the electric field spatial dependence and the antenna structure from measurements of the perturbed distribution function at a single location. With data from multiple spatial locations the function W is over-determined making the reconstruction a test of the continuum representation. Figure 8 shows a comparison of the spatial fourier transform of the plasma electric field obtained through the inverse G -transform of the velocity dependence of the data as compared to a determination from the spatial dependence of the density fluctuations. Curiously, we have more detailed information on the spatial dependence of the electric field from the velocity dependence of the data (the data sets do contain five times as many velocities as they do positions). This is emphasized more by representing the fields in space as in Fig. 9. Although the signal to noise of the measurements of f^1 is near 10^2 , there is significant degradation of the signal to noise due to cancellations in the integral of f^1 to obtain n^1 and the electric field is proportional to the spatial derivative of n^1 . The electric displacement

$D = \varepsilon E$ is related to the external charge density (the antenna) and is shown in Fig. 10. The location and periodicity of the antenna (which is very different from the periodicity of the ion acoustic wave) are clearly evident in the reconstruction. The calculation in Fig. 10 was done from data at a single spatial location.

V. COMMENTS AND CONCLUSIONS

Another feature of slightly non-Maxwellian distribution functions is that the energy density of the modes is strongly affected by fast particles. For simplicity we will consider the situation in one dimension. The energy density is given by the formula of Kruskal and Oberman:³

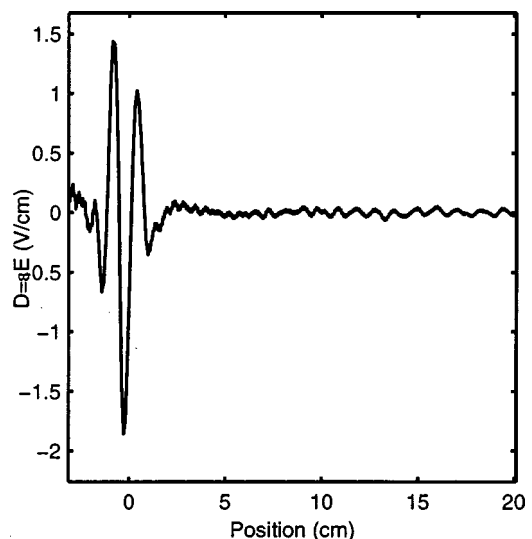


FIG. 10. Calculation of the electric displacement $D(z)$ (the external electric field) from f^1 data at a single location indicating the location and structure of the antenna.

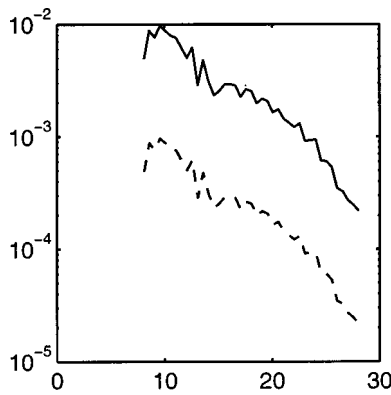


FIG. 11. Wave energy density normalized to the plasma thermal energy density as computed by Eq. (10) (solid curve) and the fluid theory (dashed curve).

$$\rho_E = \int_{-\infty}^{\infty} \frac{m_i v |f^1|^2}{-\frac{\partial f}{\partial v}} dv. \quad (10)$$

For an ion acoustic wave with $T_e \gg T_i$ and f Maxwellian, this integral produces the usual fluid theory energy density $\rho_E = n \kappa T_e |n^1/n|^2$ where n is the equilibrium ion density and n_1 is the density perturbation due to the wave. However, for the modes observed in the experiments, the energy density of the acoustic mode and of the kinetic modes are typically larger by a factor of 3 than the energy density as predicted by the fluid theory of the ion acoustic mode with the same ion distribution. The fluid theory predicts that the wave mode energy density will simply be proportional to the thermal energy density of the particles. Figure 11 shows the spatial dependence of the wave energy density calculated from the Kruskal–Oberman formula [Eq. (10)] as compared to the fluid theory for excitation at 40 KHz. We have verified that the energy density derived by Morrison in terms of the CVK mode amplitudes is identical to the result of Eq. (10) for the data.⁴

In this experiment we find that the damping of the ion perturbations can be completely explained in terms of charge exchange collisions (mean free path of 12 cm). The damping due to Coulomb collisions is weaker typically by an order of magnitude. This would not be the case for the kinetic modes if the plasma were to be Maxwellian as was discussed in our earlier work.¹

Kinetic modes form an important and potentially dominant component of the electrostatic degrees of freedom in slightly non-Maxwellian plasmas. These modes are sensitive to details in the velocity distribution function. Further work is needed to understand the dynamics of these modes in situations where the distribution functions themselves are being modified in a quasilinear fashion by the waves. Measurements of coherent three-wave interaction in phase space confirm the importance and identity of the kinetic modes.¹¹ Use of the Case–Van Kampen continuum as a basis for the representation of the plasma degrees of freedom appears to work well here despite the fact that the continuum, strictly speaking, does not exist in weakly collisional plasma.^{1,2} We believe that this seemingly paradoxical result can be under-

stood as follows. The introduction of weak collisions in a collisionless plasma is a singular perturbation that makes its presence felt over spatial (or temporal) scales long enough to allow for the development large velocity gradients in the distribution function. Although there is structure in the perturbed distribution functions, it is not at fine scales. It is thus not surprising that the collisionless theory applies to this weakly collisional experiment where the deviation of the distribution function from a Maxwellian strongly reduces the phase-mixing and consequent effects of collisions on the kinetic modes.

ACKNOWLEDGMENT

This work supported by Grant No. DE-FG02-99ER54543 from the U.S. Department of Energy.

APPENDIX: MULTI-FLUID DESCRIPTION

We can attempt to describe the appearance of kinetic modes using a three-fluid theory, with the three fluids corresponding to bulk ions, beamlike ions, and electrons. The equations of motion for the two ion species are

$$m_i n_{i,b} \left(\frac{\partial v_{i,b}}{\partial t} + v_{i,b} \frac{\partial v_{i,b}}{\partial x} \right) = e n_{i,b} E - \frac{\partial p_{i,b}}{\partial x}. \quad (A1)$$

We linearize Eq. (A1), assuming plane-wave solutions of the form $\exp[i(kx - \omega t)]$ and let $p_{i,b} = n_{i,b} T_{i,b}$ with constant temperature $T_{i,b}$. A model ion distribution function

$$g_0 = \frac{1}{(1 + \varepsilon \xi^2) \sqrt{\pi}} \{ \exp(-u^2) + \varepsilon \xi^3 \exp[-\xi^2(u - \bar{u})^2] \} \quad (A2)$$

can have the parameters adjusted so as to match the distribution function in Fig. 5. We can then solve for the perturbed densities as

$$n_{i1} = \frac{i e n_{i0} k E}{m_i \omega^2 - k^2 T_i}, \quad (A3)$$

and

$$n_{b1} = \frac{i e n_{b0} k E}{m_i (\omega - k v_{b0})^2 - k^2 T_b}. \quad (A4)$$

Assuming Boltzmann response for the ions as well as electrons, we write $n_{i1} + n_{b1} \approx n_0 e \phi_1 / T_e$, with $E = -ik \phi_1$. Using expressions (A3) and (A4), we then obtain the dispersion relation,

$$a \kappa^4 + b \kappa^3 + c \kappa^2 + d \kappa + 1 = 0, \quad (A5)$$

which is a fourth-order algebraic equation for κ with

$$a = \frac{1}{2} \left(\frac{1}{2 \xi^2} - \bar{u}^2 \right) \left(\frac{r}{\tau} + 1 \right) + \frac{1-r}{4\tau},$$

$$b = \mathbf{u}(1 + r/\tau), \quad c = \bar{u}^2 - \frac{1}{2} \left(\frac{1}{\xi^2} + 1 + \frac{1}{\tau} \right), \quad d = -2\bar{u},$$

where $r = 1/(1 + \varepsilon \xi^2)$. We solve Eq. (A5) numerically. For the case described by Fig. 2, the four roots for κ are found to be -1.003 , 0.996 , 0.600 , and 0.754 . Whereas the first two

roots are spurious and have no counterparts in the kinetic roots, the last two roots are close to the real part of the two least damped roots in Fig. 4.

While it may be satisfying to recover the real parts of the wave numbers of two weakly damped modes from the multi-fluid model described above, the model has serious limitations. First, we learn nothing from the fluid model about the damping of the modes which is essentially kinetic in origin. Second, the fluid model finds spurious modes, mentioned above, with no counterparts in the kinetic calculation. Third, it is not obvious how many beamlike ion components one should actually include in the multi-fluid model unless one has *a priori* knowledge of the kinetic spectrum. Inspection of Fig. 4 shows that there are more than two modes with weak damping rates, and yet the fluid model yields only two simply because the ion population was divided up conveniently

into one bulk and one beamlike component. Nevertheless, it is evident that for kinetic modes the ion distribution function acts like a collection of independent fluids.

¹F. Skiff, S. De Souza-Machado, W. A. Noonan, A. Case, and T. N. Good, Phys. Rev. Lett. **81**, 5820 (1998).

²C. S. Ng, A. Bhattacharjee, and F. Skiff, Phys. Rev. Lett. **83**, 1974 (1999).

³P. J. Morrison, Phys. Plasmas **1**, 1447 (1994).

⁴B. D. Fried and A. Y. Wong, Phys. Fluids **9**, 1084 (1966).

⁵I. M. A. Gledhill and M. A. Hellberg, J. Plasma Phys. **36**, 75 (1986).

⁶S. P. Gary and R. L. Tokar, Phys. Fluids **28**, 2439 (1985).

⁷R. L. Mace, G. Amery, and M. A. Hellberg, Phys. Plasmas **6**, 44 (1999).

⁸S. De Souza-Machado, M. Sarfaty, and F. Skiff, Phys. Plasmas **6**, 2323 (1999).

⁹F. Skiff, C. S. Ng, A. Bhattacharjee, W. A. Noonan, and A. Case, Plasma Phys. Controlled Fusion **42**, B27 (2000).

¹⁰H. Gunell and F. Skiff, Phys. Plasmas **8**, 3550 (2001).

¹¹A. Case, Ph.D. thesis, University of Maryland, College Park, 2001.